

- 9 Bahadur, M and Sharma, T., Abstracts of the XVI All India Cell Biology Congress and Symposium, Varanasi, 1993, pp. 1-83.
 10. Marshall, J. T., *Bull. Am Mus. Natl Hist.*, 1977, **158**, 173-220.
 11 Sabatier, M., *Palaeovertebrata*, 1982, **12**, 1-56.
 12. Black, C. C. and Krishtalka, L., *Contrib. Sci.*, 1986, **372**, 1-15.

ACKNOWLEDGEMENTS. R.P thanks CSIR New Delhi for financial support. Collection of extant species from different parts of India was partly covered by support received by TS from ICMR GSF, Germany.

Received 16 April 1993, accepted 16 July 1993

Prostatic inhibin has a predominantly anti-parallel β -sheet structure

K. V. R. Chary, Vinit K. Rastogi, Girjesh Govil, Seema V. Garde* and Anil R. Sheth*

Chemical Physics Group, Tata Institute of Fundamental Research, Homi Bhabha Road, Colaba, Bombay 400 005, India

*Institute for Research in Reproduction, Jahangir Merwanji Street, Parel, Bombay 400 012, India

Prostatic inhibin (94 amino acid residues, $M_r = 10,540$) is a protein isolated from the human and animal prostate glands. Three-dimensional structure of this cysteine-rich (10/94) protein has been studied by NMR spectroscopy. Preliminary investigations provide valuable information on the secondary structure of this protein. It is found to acquire a predominantly anti-parallel β -sheet structure and possibly the molecule is locked into several such sheets through disulphide linkages.

PROSTATIC inhibin is a protein with 94 amino acids and molecular weight of 10 kDa. It has been isolated from the human and animal prostate glands¹. More than a decade of research has established a wide range of its biological activities, ranging from preventing pregnancy to curing prostate cancer. Inhibin prevents pregnancy by modulating the level of circulating follicle-stimulating hormone (FSH) in mammals¹. It suppresses prolactin, a hormone that promotes lactation². Therefore, neutralizing inhibin through active immunization has been found to increase milk production. Although the primary structure of this molecule³ has been determined, no information is available so far about the three-dimensional structure. Our preliminary NMR investigations throw light on the three-dimensional structure of prostatic inhibin – an information of great value, in view of the useful biological activities of this molecule.

About 20 mg of HPLC pure protein⁴ was dissolved in 0.5 ml of an appropriate solvent (approximately 3 mM) and buffered with 100 mM acetate buffer. The pH was

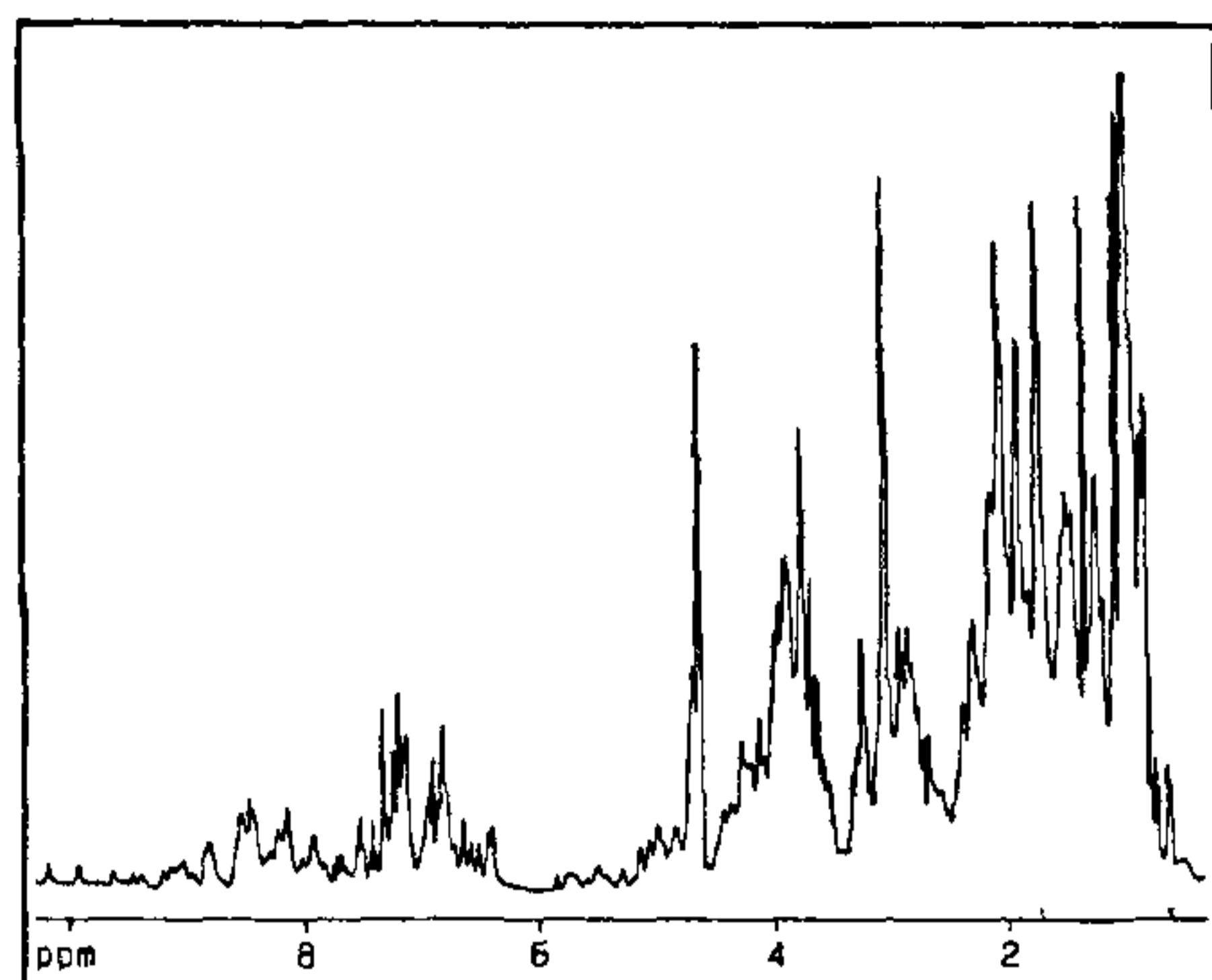


Figure 1. 500 MHz ^1H NMR spectrum of prostatic inhibin in a mixed solvent of 90% H_2O + 10% $^2\text{H}_2\text{O}$ at 310 K and pH 4.2 (acetate buffer).

adjusted to 4.2. NMR measurements were carried out in 99.9% $^2\text{H}_2\text{O}$ and in a mixed solvent consisting of 90% H_2O and 10% $^2\text{H}_2\text{O}$. Temperature was optimized for the best possible resolution and all spectra were recorded at 310 K. NMR experiments were carried out on a Bruker AMX 500 spectrometer with a ^1H frequency of 500 MHz and involve (i) two-dimensional (2D) two-quantum-filtered correlation spectroscopy (2QF COSY)⁵, (ii) 2D clean total correlation spectroscopy (clean TOCSY)⁶ with a mixing time of 100 ms, and (iii) 2D nuclear Overhauser enhancement spectroscopy (NOESY)⁷.

Prostatic inhibin has about 600 observable protons. The 500 MHz NMR spectrum shows reasonably well resolved features. Figure 1 shows the 1D ^1H spectrum of the protein in a mixed solvent of 90% H_2O and 10% $^2\text{H}_2\text{O}$. Figure 2A and 2B show 2QF COSY and NOESY spectra, respectively, in 99.9% $^2\text{H}_2\text{O}$. A detailed analysis of these and other spectra has enabled us to identify several spin systems. These include eight threonines, five valines, two glycines, one leucine, one isoleucine and twenty-one AMX spin systems (belonging to Cys, Ser, Asp, Asn, Tyr, Trp, His and Phe). The subspectral features are well dispersed. For example, the $\text{C}_\beta\text{H}-\text{C}_\gamma\text{H}_3$ correlations for all the eight threonine residues present in the prostatic inhibin are shown in Figure 3. Thus, at this stage, we have been able to identify almost half of the spin systems. Even in the absence of sequential resonance assignments, the NMR data provide valuable information on the secondary structure of this protein.

In the first instance, the 1D spectrum (Figure 1) indicates that the protein has a well-defined and ordered structure. There are several downfield-shifted C_αH protons as well as several upfield-shifted methyl resonances. The downfield shift of the C_αH protons is a

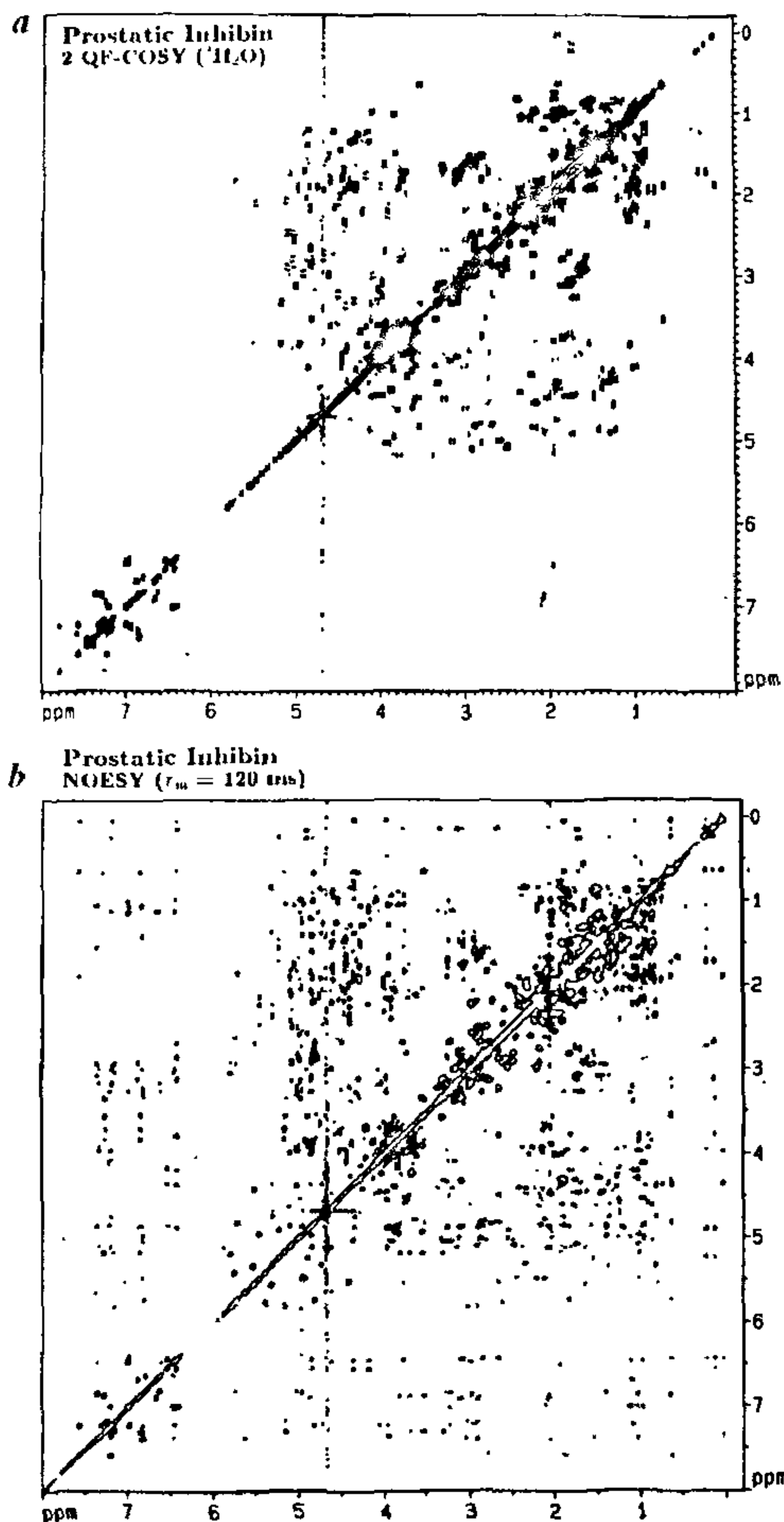


Figure 2. *a*, 2QF COSY spectrum of prostatic inhibin in 99.9% $^2\text{H}_2\text{O}$ at 310 K and pH 4.2 (acetate buffer). Experimental parameters: $t_{1\text{max}} = 65.4$ ms, $t_{2\text{max}} = 409.6$ ms; recycle delay = 1 s; 96 scans/ t_1 increment; time domain data points, 654 and 4096 along t_1 and t_2 dimensions, respectively. The ^1H carrier frequency was on the water resonance. The data were multiplied with unshifted sine-bell window functions along both the axes and zero-filled to 2048 along the t_1 dimension prior to 2D FT. The digital resolution along ω_1 and ω_2 corresponds to 4.88 and 2.44 Hz/point, respectively. *b*, Pure absorption 2D NOESY spectrum of prostatic inhibin in 99.9% $^2\text{H}_2\text{O}$. Experimental parameters: $t_{1\text{max}} = 60.0$ ms, mixing time (τ_m) = 120 ms; 128 scans/ t_1 increment; time domain data points, 600 and 4096 along t_1 and t_2 dimensions, respectively. The data were multiplied with sine-bell window functions shifted by $\pi/4$ and $\pi/8$ along t_1 and t_2 axes, respectively, and zero-filled to 2048 data points along the t_1 dimension prior to 2D FT. Other experimental and processing parameters were the same as in the case of 2QF COSY.

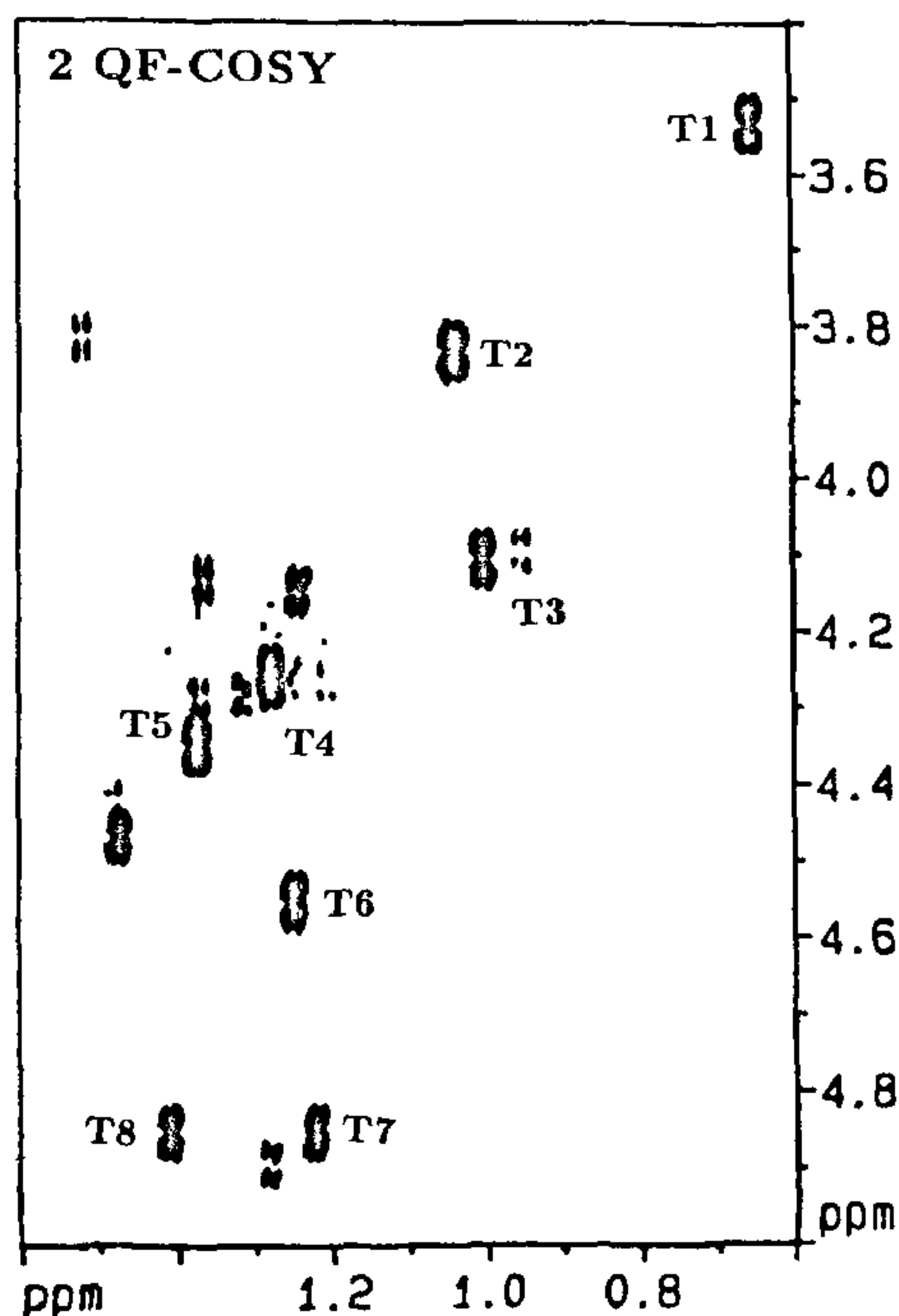


Figure 3. Selected region of 2QF COSY spectrum (Figure 2*a*) of prostatic inhibin showing through-bond correlations from C_βH protons to $\text{C}_\gamma\text{H}_3$ protons for all the eight threonine residues in prostatic inhibin.

direct consequence of the deshielding effect of hydrogen bonds in their vicinity. The upfield shift of methyl resonances can be attributed to an interaction between different methyl resonances in close vicinity in the hydrophobic core of the protein. Several amide (NH) protons in the protein are well shielded from water and exchange very slowly with $^2\text{H}_2\text{O}$.

The cross-peaks in NOESY spectra arise from short interproton distances (typically < 0.4 nm) and throw light on the secondary structure of the protein⁸. There are several diagnostic features for establishing the secondary structure of a protein by NMR. For example, in α -helices the sequential NH-NH distances (d_{NN}) are short (< 0.28 nm), giving rise to strong d_{NN} cross-peaks in NOESY spectra. Such d_{NN} contacts are not seen in parallel or anti-parallel β -sheets. However, in the presence of β -sheet segments of either type, one observes strong $\text{C}_\alpha\text{H-NH}$ ($d_{\alpha\text{N}}$) cross-peaks in NOESY spectra as the distance between C_αH of the i th amino

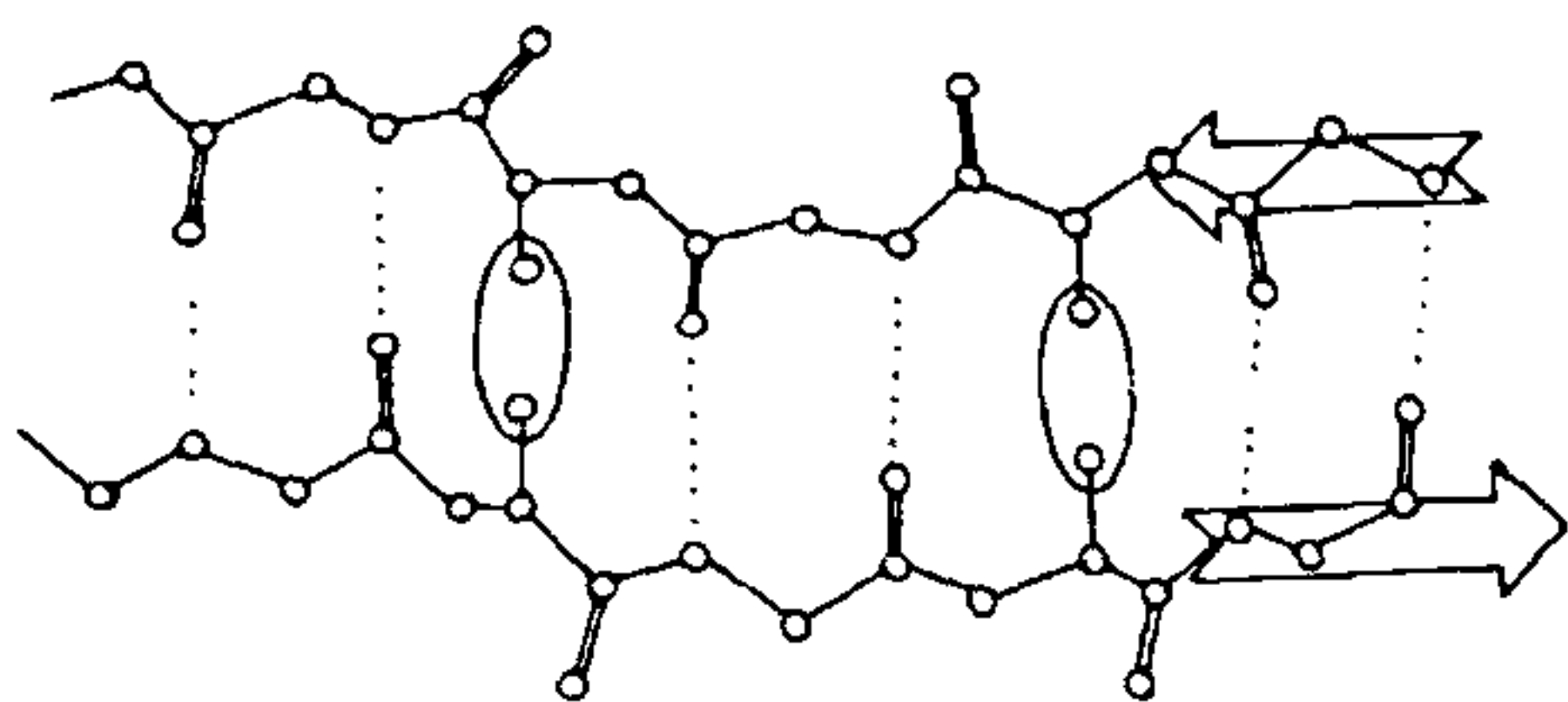


Figure 4. Schematic diagram of anti-parallel β -sheet depicting the $C_{\alpha}H-C_{\alpha}H$ contacts (identified by ellipses between the strands)

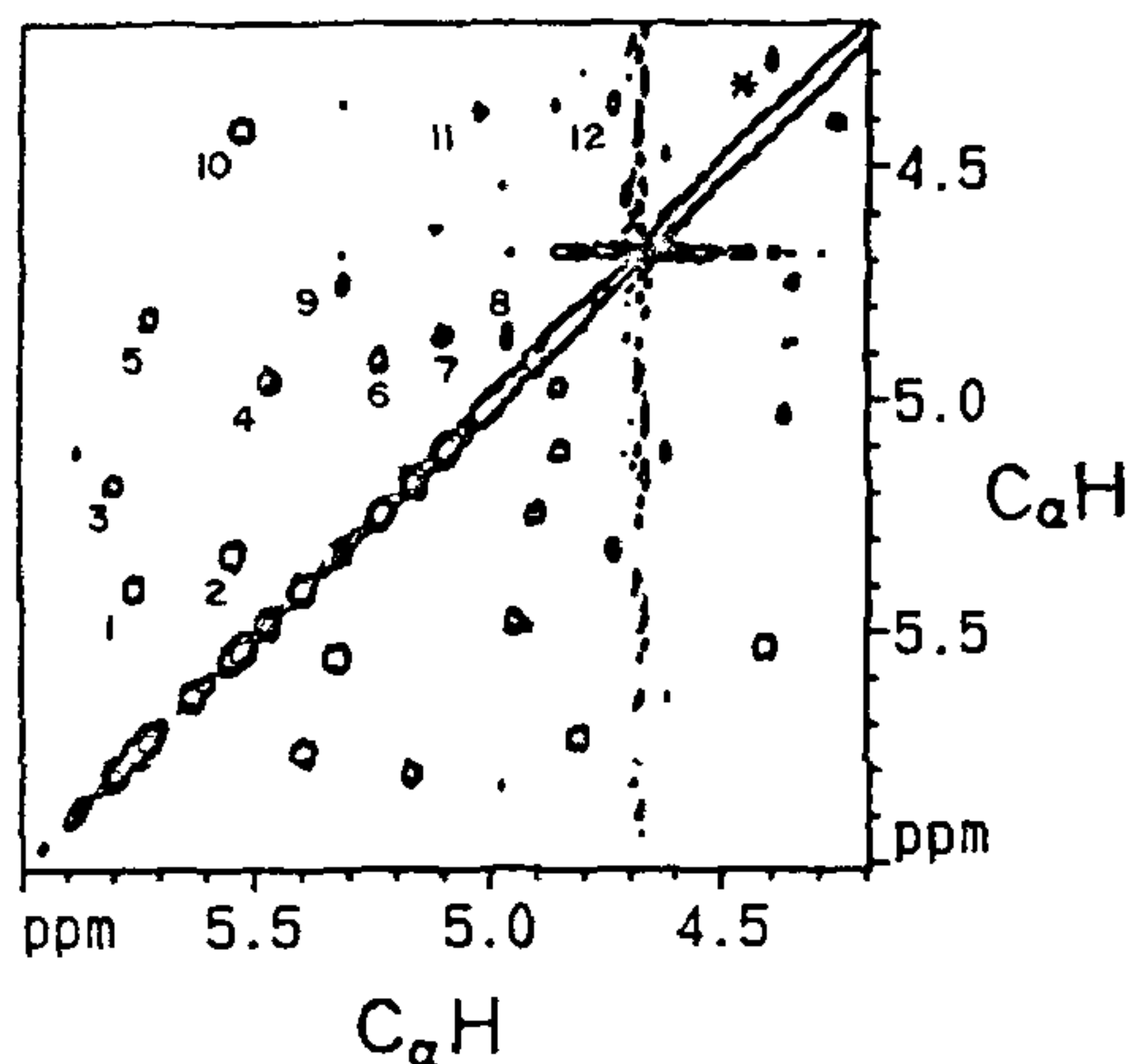


Figure 5. Selected region of the NOESY spectrum (Fig 2b) of prostatic inhibin showing nOe connectivities between various $C_{\alpha}H$ protons. The $C_{\alpha}H-C_{\alpha}H$ contacts are explicitly numbered. The peak identified with an asterisk is the nOe between $C_{\alpha}H$ and $C_{\beta}H$ protons belonging to one of the threonine residues in prostatic inhibin.

acid residue and NH of the $(i+1)$ st residue is short (< 0.22 nm). To distinguish between parallel and anti-parallel β -sheet(s), one monitors long-range ($C_{\alpha}H-C_{\alpha}H$) contacts. The distance between two $C_{\alpha}H$'s belonging to the two strands of an anti-parallel β -sheet is less than 0.23 nm, giving rise to a strong $C_{\alpha}H-C_{\alpha}H$ cross-peak in NOESY spectra. In the case of parallel β -sheet, $C_{\alpha}H-C_{\alpha}H$ contacts are not observed because such distances are larger than 0.48 nm. Thus, the presence or absence of the above-mentioned cross-peaks in NOESY spectra can be attributed to the presence or absence of these three characteristic polypeptide segments, which form an integral part of most of the proteins.

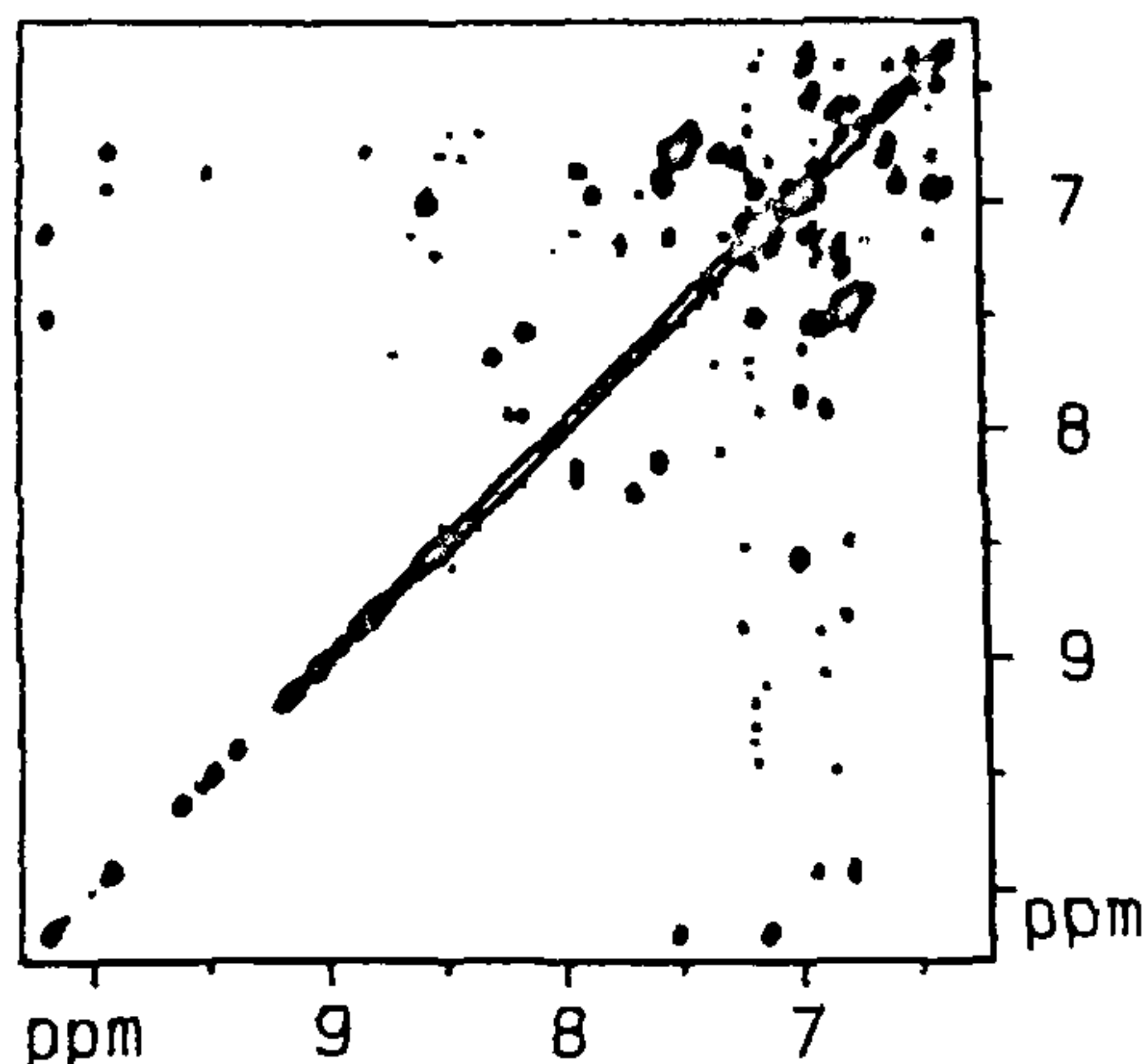


Figure 6. Selected region of the pure absorption 2D NOESY spectrum of prostatic inhibin in a mixed solvent of 90% H_2O + 10% 2H_2O at 310 K and pH 4.2 (acetate buffer). Experimental parameters were as follows: $t_{1max} = 48.4$ ms, $t_{2max} = 360.0$ ms; mixing time (τ_m) = 150 ms; recycle delay = 1 s; 144 scans/ t_1 increment, time domain data points, 550 and 4096 along t_1 and t_2 dimensions, respectively. The 1H carrier frequency was on the water resonance. The data were multiplied with sine-bell window functions shifted by $\pi/4$ and $\pi/8$ along t_1 and t_2 axes, respectively and zero-filled to 1024 data points along the t_1 dimension prior to 2D FT. The digital resolution along ω_1 and ω_2 corresponds to 11.09 and 5.54 Hz/point, respectively.

As illustrated in Figure 4, the presence of two strands of five amino acid residues each in anti-parallel conformation results in two $C_{\alpha}H-C_{\alpha}H$ contacts. In the case of prostatic inhibin, the NOESY spectrum (Figure 5) reveals at least twelve $C_{\alpha}H-C_{\alpha}H$ contacts, providing a direct evidence for the presence of extensive anti-parallel β -sheet segment(s). One can make an estimate of the total number of amino acids involved in such a structure, corresponding to a minimum of twelve $C_{\alpha}H-C_{\alpha}H$ contacts, for certain model situations, for example: (i) two anti-parallel strands of twenty-five amino acids each; (ii) six pairs of anti-parallel strands, where each strand is made up of five amino acids; (iii) three anti-parallel β -sheets, each one with three anti-parallel strands of five amino acids each, etc. These illustrative examples show that the total number of amino acids participating in anti-parallel β -sheet conformations may range between 50 and 70. On the other hand, examination of the NOESY spectrum in the mixed solvent (90% H_2O + 10% 2H_2O) shows very few d_{NN} connectivities (Figure 6). This indicates a virtual absence of α helical structures, which are characterized by short d_{NN} connectivities. In anti-parallel β -sheet(s) the d_{NN} 's are approximately

0.50 nm. Hence, one would not see such contacts in NOESY spectra.

Thus, we conclude that prostatic inhibin acquires a predominantly anti-parallel β -sheet structure and possibly the molecule is locked into several such sheets through disulphide linkages.

1. Garde, S., Sheth, A. R., Lohiyaa, N. K. and Shah, M. G., *J. Biosci.*, 1992, **17**, 67-85.
2. Moodbidri, S. B., Hurkadli, K. S. and Sheth, A. R., *Ind J Exp Biol.*, 1989, **27**, 214-216.
3. Seidah, N. G., Arbatti, N. J., Rochemont, J., Sheth, A. R. and Chretien, M., *FEBS Lett.*, 1984, **175**, 349-355.
4. Vanage, G. R., Garde, S., Sheth, A. R. and Gopalakrishnan, K., *Int. J. Androl.*, 1992, **15**, 114-126.
5. Piantini, U., Sorensen, O. W. and Ernst, R. R., *J. Am. Chem. Soc.*, 1982, **104**, 6800-6801.
6. Griesinger, C., Otting, G., Wuthrich, K. and Ernst, R. R., *J. Am. Chem. Soc.*, 1988, **110**, 7870-7872.
7. Kumar, A., Wagner, G., Ernst, R. R. and Wuthrich, K., *Biochem. Biophys. Res. Commun.*, 1980, **96**, 1156-1163.
8. (a) Ernst, R. R., *Angew. Chem. Int. Ed. Engl.*, 1992, **31**, 805-823
(b) Wuthrich, K., *Science*, 1989, **243**, 45-50.

ACKNOWLEDGEMENTS Use of the facilities provided by 500 MHz FT NMR National Facility supported by the Department of Science and Technology, Government of India and located at T. I. F. R., Bombay, and the preliminary experiments done by Priya Chandran under Visiting Students Research Programme of T. I. F. R., are gratefully acknowledged.

Received 3 May 1993; revised accepted 24 June 1993

Cisplatin and ascorbic acid: Synergistic antitumour effect against Dalton's lymphoma in mice

Suniti Sarna and R. K. Bhola

Department of Zoology, Gauhati University, Guwahati 781 014, India

Therapeutical potential of low dose of cisplatin alone or in combination with ascorbic acid was studied in C₃H/He mice bearing Dalton's lymphoma. Sub-therapeutical dose of cisplatin (3 mg/kg) was able to increase the survival time of tumour-bearing mice without any tumour-free survivor. Ascorbic acid enhances the antitumour effect of cisplatin, resulting in increased life span of tumour-bearing mice as well as tumour-free survivors. The enhancement of cisplatin-induced tumour growth inhibition by ascorbic acid is probably due to the modulation of permeability of tumour cell membrane which increases the uptake of cisplatin into the tumour cells.

A number of side effects of cisplatin like nephrotoxicity, ototoxicity, neuropathy and myelosuppression

are widely described in various animals as well as in humans¹⁻⁷. Cisplatin-induced renal toxicity is the main limiting factor for its clinical use and can be partially reduced by pretreatment hydration and administration of furosemide and/or mannitol⁸, sodium 2-mercaptoethane sulfonate^{9, 10}, nicotinamide or 3-amino-benzamide¹¹ and selenium¹². It is often not possible to successfully treat tumours by increasing the dose level of cisplatin because such therapy may be fatally toxic though it reduces the tumour burden significantly^{12, 13}. Thus combination therapy with an agent which enhances the antitumour effect of cisplatin with little or no enhancement of cisplatin's toxicity is of value in the treatment of various tumours that fail to respond to treatment with cisplatin alone. It has been reported that nifedipine enhances the antitumour effect of cisplatin (4 mg/kg) against the cisplatin-sensitive murine amelanotic melanoma as well as Lewis lung carcinoma^{13, 14}. Recently it has been reported that therapeutical potential of low dose of cisplatin (3 mg/kg) against Dalton's lymphoma is greatly enhanced when it is used in combination with glucose^{15, 16}. The present studies were undertaken to determine the combined effect of ascorbic acid and cisplatin on the growth of Dalton's lymphoma in mice in order to find out the effect of ascorbic acid on enhancement of tumour growth inhibition induced by a low dose of cisplatin.

C₃H/He strain of mice-bearing Dalton's lymphoma originally procured from the Chittaranjan National Cancer Research Institute, Calcutta and maintained in the laboratory by regular serial transplantations was used in all sets of experiments. The day of tumour transplantation was taken as day 0. On the 6th day mice-bearing palpable tumour was treated i.p. with 4 repeated injections of either 20, 40 or 60 mg/kg of ascorbic acid. The injections were administered on alternate days. The survival period of tumour-bearing mice and the percentage of tumour-free survivors were observed in each group (10 mice in each group). For combination therapy cisplatin was dissolved freshly in balanced salt solution. Different groups of mice were treated with single i.p. injection of subtherapeutical dose of cisplatin (3 mg/kg) along with repeated injections of ascorbic acid (20, 40 or 60 mg/kg). Cisplatin was injected on 6th day following tumour transplantation. On the same day a single injection of ascorbic acid (20, 40 or 60 mg/kg) was also given followed by three repeated injections of ascorbic acid on alternate days. The mean survival time of tumour-bearing mice and the percentage of tumour-free survivors were studied in each group of mice. In the experimental batch, the percentage of increased life span was calculated by the following formula¹⁷

Percentage of increased life span = $[(T - C)/C] \times 100$;
T = mean survival time of treated mice, C = mean survival time of untreated control mice.